

High-quality $\text{InAs}_y\text{P}_{1-y}$ step-graded buffer by molecular-beam epitaxy

M. K. Hudait and Y. Lin

Department of Electrical Engineering, The Ohio State University, Columbus, Ohio 43210

D. M. Wilt

NASA Glenn Research Center, Cleveland, Ohio 44135

J. S. Speck

Department of Materials Science, University of California, Santa Barbara, California 93106

C. A. Tivarus, E. R. Heller, and J. P. Pelz

Department of Physics, The Ohio State University, Columbus, Ohio 43210

S. A. Ringel^{a)}

Department of Electrical Engineering, The Ohio State University, Columbus, Ohio 43210

(Received 11 November 2002; accepted 13 March 2003)

Relaxed, high-quality, compositionally step-graded $\text{InAs}_y\text{P}_{1-y}$ layers with an As composition of $y=0.4$, corresponding to a lattice mismatch of $\sim 1.3\%$ were grown on InP substrates using solid-source molecular-beam epitaxy. Each layer was found to be nearly fully relaxed observed by triple axis x-ray diffraction, and plan-view transmission electron microscopy revealed an average threading dislocations of $4 \times 10^6 \text{ cm}^{-2}$ within the $\text{InAs}_{0.4}\text{P}_{0.6}$ cap layer. Extremely ordered crosshatch morphology was observed with very low surface roughness (3.16 nm) compared to cation-based $\text{In}_{0.7}\text{Al}_{0.3}\text{As}/\text{In}_x\text{Al}_{1-x}\text{As}/\text{InP}$ graded buffers (10.53 nm) with similar mismatch and span of lattice constants on InP. The results show that $\text{InAs}_y\text{P}_{1-y}$ graded buffers on InP are promising candidates as virtual substrates for infrared and high-speed metamorphic III–V devices.
© 2003 American Institute of Physics. [DOI: 10.1063/1.1572476]

$\text{InAs}_y\text{P}_{1-y}$ alloys are of interest for both infrared optoelectronic and high-speed electronic device applications due to their wide range of band-gap energies from 0.36 eV to 1.35 eV and the large band offset energies possibly using $\text{InAs}_y\text{P}_{1-y}/\text{In}_x\text{Ga}_{1-x}\text{As}$ heterostructures grown on InP.^{1–3} $\text{InAs}_y\text{P}_{1-y}$ alloys are also of interest for compositionally graded buffer applications, where the span of lattice constants between InP and InAs provides the opportunity for generating “virtual substrates” on InP to support a wide variety of lattice-mismatched devices based on $\text{In}_x\text{Ga}_{1-x}\text{As}$, $\text{In}_x\text{Al}_{1-x}\text{As}$, and $\text{InAs}_y\text{P}_{1-y}$. This is currently being explored for thermophotovoltaic (TPV) devices based on $\text{In}_x\text{Ga}_{1-x}\text{As}$, where the band gaps required for optimal TPV system conversion efficiencies in the range of 0.5–0.6 eV necessitate $\text{In}_x\text{Ga}_{1-x}\text{As}$ compositions ($x=0.69–0.81$) that generate a significant lattice mismatch with respect to the InP substrate.^{4–7} The use of an anion (group-V)-based alloy, such as $\text{InAs}_y\text{P}_{1-y}$ for compositionally graded buffers, compared with more common graded buffer alloy choices, such as $\text{In}_x\text{Ga}_{1-x}\text{As}$ and $\text{In}_x\text{Al}_{1-x}\text{As}$, which can also bridge the lattice constant mismatch between active device layers and the InP substrate, offers a potential advantage since control of the growth rate (indium flux) is decoupled from control of the layer composition (As:P flux ratio). The addition of the group-V sublattice, as an independently controlled variable, has the effect of widening the parameter space for the growth of such graded buffers that is otherwise constrained for cation (group-III)-based graded buffers where growth rates and compositions are both dictated by the group-III sources. This

is particularly advantageous for solid-source molecular-beam epitaxy (MBE) growth since optimizing the group-III fluence with respect to both composition and growth rate is extremely time consuming and would require substantial growth interruptions that may compromise interface quality. In this letter, we report the growth of high-quality relaxed $\text{InAs}_y\text{P}_{1-y}$ step-graded buffers by solid-source MBE that show great promise for virtual substrates applications.

$\text{InAs}_y\text{P}_{1-y}$ compositionally step-graded (four steps) layers with As mole fractions (y) from 0.05 to 0.40 were grown on (100) semi-insulating InP substrates using solid-source MBE equipped with valved cracker sources for arsenic and phosphorus. Substrate oxide desorption was done at 510 °C under a phosphorus overpressure of $\sim 1 \times 10^{-5}$ Torr, which was confirmed by the observation of a strong (2×4) reflection high-energy electron diffraction (RHEED) pattern, indicative of a clean (100) InP surface. An initial 0.2 μm thick undoped InP buffer layer was then deposited to generate a smooth surface at ~ 485 °C under a stabilized P_4 flux prior to the growth of $\text{InAs}_y\text{P}_{1-y}$ step-graded buffers. After InP growth, the P_4 flux was reduced to the required value for the $\text{InAs}_y\text{P}_{1-y}$ growth and the As valve was opened before introducing In into the growth chamber. The exposure time of As on the InP surface was minimized in order to avoid the formation of an InAsP interlayer due to As–P exchange on the InP surface.^{8,9} For all $\text{InAs}_y\text{P}_{1-y}$ layers, the growth rate was 0.75 monolayers/s, as determined by RHEED intensity oscillations at a constant substrate temperature of 485 °C controlled by a pyrometer-based feedback control system. The first three undoped step-graded layers were each grown to a thickness of 0.4 μm , followed by a 1.7 μm thick n -type (Si-doped) $\text{InAs}_{0.4}\text{P}_{0.6}$ layer with $n \sim 3 \times 10^{16} \text{ cm}^{-3}$ for char-

^{a)}Author to whom correspondence should be addressed; electronic mail: ringel@ee.eng.ohio-state.edu

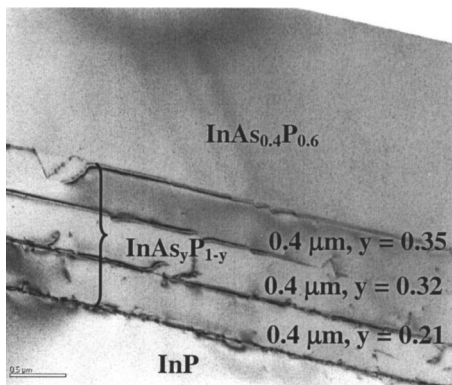


FIG. 1. Cross-sectional TEM image of $\text{InAs}_{0.4}\text{P}_{0.6}$ structure grown on (100) InP substrate using $\text{InAs}_y\text{P}_{1-y}$ step-graded buffers.

acterization purposes. The total mismatch between the cap layer and the InP substrate is $\sim 1.3\%$.

Figure 1 shows a cross-sectional transmission electron microscopy (XTEM) image of a typical $\text{InAs}_{0.4}\text{P}_{0.6}/\text{InAs}_y\text{P}_{1-y}/\text{InP}$ step-graded buffer structure. The compositions shown in Fig. 1 were determined using triple axis x-ray diffraction (described below). The image of Fig. 1 shows a high contrast at the graded buffer layer interfaces due to misfit dislocations with no threading dislocations (TDs) observable in the $1.7 \mu\text{m}$ thick $\text{InAs}_{0.4}\text{P}_{0.6}$ cap layer using XTEM. Hence, to accurately quantify the dislocation density, plan-view transmission electron microscopy (TEM) measurements were performed, the results of which are shown in Fig. 2. By considering several fields of view, the average TD density (TDD) in the relaxed $\text{InAs}_{0.4}\text{P}_{0.6}$ cap was found to be $4 \times 10^6 \text{ cm}^{-2}$. It should be noted that both etch pit density (EPD) measurements using $\text{AgNO}_3:\text{CrO}_3:\text{HF}:\text{H}_2\text{O}$ (A-B etch) and electron-beam-induced current measurements on InGaAs p - n junctions grown on the InAsP buffer were also performed. These measurements revealed matching values of $\sim 1 \times 10^5 \text{ cm}^{-2}$ for EPD and dark spot density, respectively, in substantial disagreement with the plan-view TEM results and significantly underestimating the true TDD value. This exemplifies the general difficulty in quantifying TDD values in high-quality relaxed buffers.

The relaxation state of the $\text{InAs}_y\text{P}_{1-y}$ graded buffer structure was evaluated using high-resolution triple axis x-ray diffraction measurements. Figure 3 shows reciprocal space maps (RSMs) for the (004) and (224) reflections. From

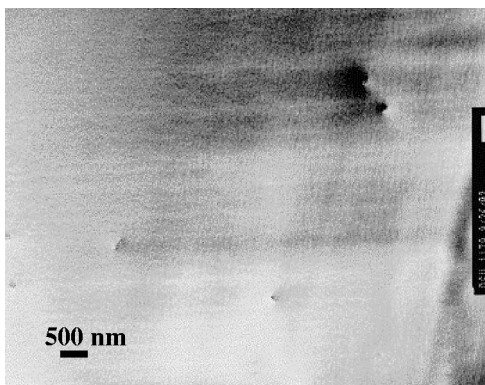


FIG. 2. Plan-view TEM micrograph of $\text{InAs}_{0.4}\text{P}_{0.6}$ layer grown on step-graded $\text{InAs}_y\text{P}_{1-y}$ buffers.

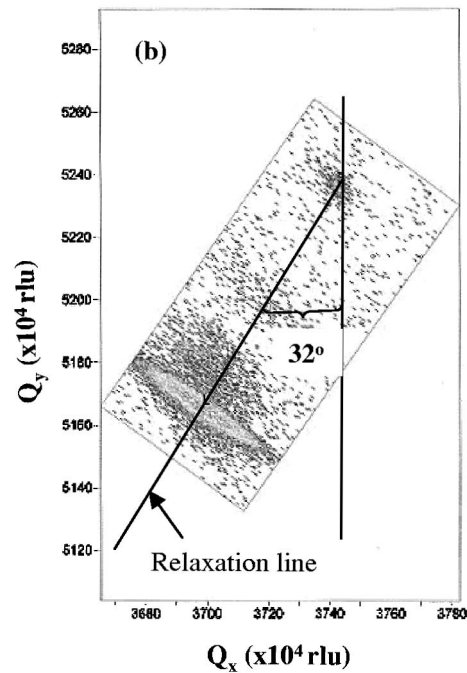
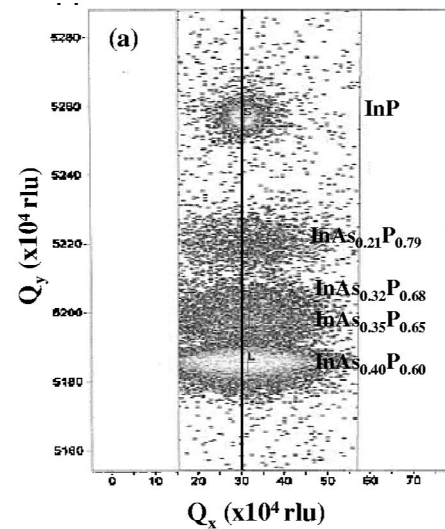


FIG. 3. (a) Symmetric (004) and (b) asymmetric (224) reciprocal space maps of $\text{InAs}_{0.4}\text{P}_{0.6}$ layer grown on InP substrate using a four-step $\text{InAs}_y\text{P}_{1-y}$ layer, showing that all of the layers are almost fully relaxed. Q_x coordinates are linked to the lattice parameter parallel to the layer plane a_{\parallel} by $Q_x = 2\lambda/(\lambda 2a_{\parallel})$, Q_y coordinates are linked to the lattice parameter perpendicular to the layer plane a_{\perp} by $Q_y = 2\lambda/a_{\perp}$. Q_x and Q_y are expressed in terms of reciprocal lattice units. Here, λ is the x-ray wavelength.

the RSM in Fig. 3(a), the diffraction intensity maximum for each layer in the buffer is almost centered on the substrate reciprocal lattice point (along the vertical line drawn here), indicating minimum lattice tilt with respect to the substrate. For the asymmetric (224) reflection in Fig. 3(b), the intensity contours corresponding to the step-graded buffer and the final $1.7 \mu\text{m}$ layer makes an angle of $\sim 32^\circ$ with respect to the substrate reciprocal lattice intensity contours indicating that the material is almost fully relaxed, since the angle between (004) and (224) is $\sim 35^\circ$. To further quantify the relaxation of each layer, the lattice parameters in the growth plane a_{\parallel} , and in the growth direction a_{\perp} , were determined. The relaxed lattice constant, a_{layer} and the relaxation, R of the layers were evaluated using¹⁰

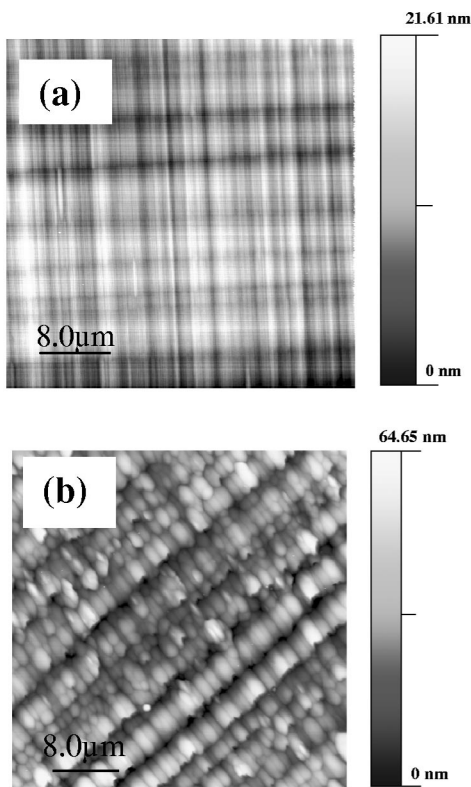


FIG. 4. AFM images from the surface of (a) $\text{InAs}_{0.4}\text{P}_{0.6}$ layer grown on InP substrate using a four-step $\text{InAs}_y\text{P}_{1-y}$ layer and (b) $\text{In}_{0.7}\text{Al}_{0.3}\text{As}$ layer grown on InP substrate using a five-step $\text{In}_x\text{Al}_{1-x}\text{As}$ layer. The scan area and the rms roughness were $40\ \mu\text{m} \times 40\ \mu\text{m}$ 3.16 nm, and 10.53 nm, respectively. Total mismatch is 1.2% and layers are more than 80% relaxed.

$$a_{\text{layer}} = (2C_{12}a_{\parallel} + C_{11}a_{\perp}) / (2C_{12} + C_{11}), \quad (1)$$

$$R = (a_{\parallel} - a_o) / (a_{\text{layer}} - a_o). \quad (2)$$

In these expressions, a_o is the InP substrate lattice parameter, and C_{11} and C_{12} are the elastic constants of each ternary $\text{InAs}_y\text{P}_{1-y}$ layer obtained using Vegard's law and the elastic constants of InP and InAs.² From the RSM data in Fig. 3, the percent relaxation was determined to be >99%, 98%, 97%, and 93% for the $\text{InAs}_{0.21}\text{P}_{0.79}$, $\text{InAs}_{0.32}\text{P}_{0.68}$, $\text{InAs}_{0.35}\text{P}_{0.65}$, and $\text{InAs}_{0.4}\text{P}_{0.6}$ layers in the buffer stack, respectively, noting an experimental error of $\pm 3\%$. This level of relaxation is consistent with the thickness of each layer being well in excess of their respective critical thicknesses, and indicates efficient relaxation of the 1.3% total misfit strain.

The most distinctive feature of $\text{InAs}_y\text{P}_{1-y}$ graded buffer, however, is the surface morphology. Figure 4(a) shows a typical atomic force microscopy (AFM) image of the relaxed $\text{InAs}_{0.4}\text{P}_{0.6}$ surface. The expected crosshatch morphology that is characteristic of strain relaxation using compositionally graded buffers¹¹⁻¹³ is clearly evident. However, compared to graded buffers consisting of cation-based grades on InP such as $\text{In}_x\text{Al}_{1-x}\text{As}$ (Ref. 14) or $\text{In}_x\text{Ga}_{1-x}\text{As}$,⁷ grown to span the identical range of lattice constant and strain on InP, the $\text{InAs}_y\text{P}_{1-y}$ surface is far superior with respect to root-mean-square (rms) roughness, peak-to-valley height, and uniformity. For comparison, Fig. 4(b) shows an AFM image of the surface of an $\text{In}_x\text{Al}_{1-x}\text{As}$ graded buffer stack comprised of $\text{In}_{0.7}\text{Al}_{0.3}\text{As}/\text{In}_x\text{Al}_{1-x}\text{As}/\text{InP}$, which incorporates almost the

same total misfit (1.2%) over the identical range of lattice constants, was found to be greater than 80% relaxed with a TDD less than $10^7\ \text{cm}^{-2}$. A detailed investigation comparing the structural properties of these buffers is beyond the scope of this letter and is the subject of a separate publication.¹⁴ Nevertheless, it is clear that the InAsP buffer results in much more ordered crosshatch and a far less granular background superimposed over the crosshatch. Analyzing the AFM data reveals a rms roughness that is more than three times lower, 3.16 nm, for the InAsP graded buffer as opposed to more than 10.53 nm for the graded InAlAs structure. The peak-to-peak roughness difference is even more dramatic due to the poor uniformity for the InAlAs structure. The vastly improved surface morphology for the InAsP graded buffer is believed to be due to advantages of grading the mole fraction of the group-V sublattice, which neither influence growth rate nor require temperature changes for MBE growth, hence providing an extra degree of freedom compared to grading on the group-III sublattice. Detailed investigations on this comparison and reporting of device performance as a function of graded buffer type are the subjects of forthcoming publications.

In conclusion, relaxed high-quality compositionally step-graded $\text{InAs}_y\text{P}_{1-y}$ layers with As compositions of $y=0.4$, corresponding to a lattice mismatch of $\sim 1.3\%$ were grown on InP substrates using solid-source MBE. Plan-view TEM revealed an average TDD of $4 \times 10^6\ \text{cm}^{-2}$. An extremely ordered crosshatch morphology was observed with very low surface roughness compared to cation-based graded buffers with a similar mismatch on InP. Hence, MBE-grown $\text{InAs}_y\text{P}_{1-y}$ step-graded buffers hold great promise as a virtual substrate technology for InP-based infrared devices.

This work is supported in part by a National Science Foundation Focused Research Group (FRG) grant (No. DMR-0076362).

- ¹M. Beaudoin, A. Bensaada, R. Leonelli, P. Desjardins, R. A. Masut, L. Isnard, A. Chennouf, and G. L'Espérance, *Phys. Rev. B* **53**, 1990 (1996).
- ²I. Vurgaftman, J. R. Meyer, and L. R. Ram-Mohan, *J. Appl. Phys.* **89**, 5815 (2001).
- ³R. P. Schneider Jr. and B. W. Wessels, *J. Electron. Mater.* **20**, 1117 (1991).
- ⁴M. W. Wanlass, J. J. Carapella, A. Duda, K. Emery, L. Gedvilas, T. Moriarty, S. Ward, J. D. Webb, X. Wu, and C. S. Murray, *AIP Conf. Proc.* **460**, 132 (1999).
- ⁵N. S. Fatemi, D. M. Wilt, R. W. Hoffman, Jr., M. A. Stan, V. G. Weizer, P. P. Jenkins, O. S. Khan, C. S. Murry, D. Scheiman, and D. J. Brinker, *AIP Conf. Proc.* **460**, 121 (1999).
- ⁶T. J. Coutts, *Renewable and Sustainable Energy Rev.* **3**, 77 (1999).
- ⁷M. W. Wanlass, J. S. Ward, K. A. Emery, M. M. Al-Jassim, K. M. Jones, and T. J. Coutts, *Sol. Energy Mater. Sol. Cells* **41**, 405 (1996).
- ⁸G. Hollinger, D. Gallet, M. Gendry, C. Santinelli, and P. Viktorovitch, *J. Vac. Sci. Technol. B* **8**, 832 (1990).
- ⁹J. M. Moiser, M. Bensoussan, and F. Honzay, *Phys. Rev. B* **34**, 2018 (1986).
- ¹⁰M. Fatemi and R. E. Stahlbush, *Appl. Phys. Lett.* **58**, 825 (1991).
- ¹¹E. A. Fitzgerald, Y.-H. Xie, M. L. Green, D. Brasen, A. R. Kortan, J. Michel, Y.-J. Mii, and B. E. Weir, *Appl. Phys. Lett.* **59**, 811 (1991).
- ¹²E. A. Fitzgerald, Y.-H. Xie, D. Monroe, P. J. Silverman, J. M. Kuo, A. R. Kortan, F. A. Thiel, and B. E. Weir, *J. Vac. Sci. Technol. B* **10**, 1807 (1992).
- ¹³J. S. Speck, M. A. Brewer, G. Beltz, A. E. Romanov, and W. Pompe, *J. Appl. Phys.* **80**, 3808 (1996).
- ¹⁴M. K. Hudait, Y. Lin, C. A. Tivarus, E. R. Heller, J. P. Pelz, J. S. Speck, and S. A. Ringel (unpublished).